# Influence of Electrode Geometry on Growth of TiNTs on Dental Implants

*ME6110 - Nanofabrication Processes*


| | |
|---|---|
| Daniel Gracias | 200110029 |
| Darshan Mali | 200110030 |
| Soham Joshi | 200110051 |

Guided by Dr Rakesh Mote

*Indian Institute of Technology Bombay, Mumbai, India*


November 2023

## Contents

Titanium and Titanium alloys are widely used for biomedical applications like dental implants due to their biocompatibility, corrosion resistance, low density and high strength. These properties arise from the oxide layer that grows naturally on the surface. By controlling the growth morphology of this oxide layer, we can significantly enhance the properties of the implants. In this paper we have attempted to study the current density spread over the surface of a dental implant in order to study the growth morphology of the Titania nanotubes on the surface of the implant. We have studied the effect of changing the parameters like shape, number and orientation of the electrodes and the voltage applied.

# 1 Introduction

Titanium and Titanium alloys exhibit good biocompatibility, high resistance to corrosion, low density and sufficient mechanical strength, making them ideal for use in dental and orthopaedic implants and other biomedical purposes. The spontaneous formation of the oxide on its surface is said to be the main reason for the same.[1] One of the biggest challenges in their use is optimization of the surface oxide properties to facilitate favourable interactions with the host tissue. The oxide layer protects the metal from corrosion, is stable and promotes osseointegration. [5]

As a consequence, great efforts have been made to stabilize and thicken this oxide layer. One of the methods to achieve this is by the formation of Titania Nanotubes (TNTs) via annodization. This significantly increases cell adhesion and also promotes in vivo bone formation. [3] The surface oxide properties can be modified by changing the electrochemical growth behaviour which depends upon various process parameters like the forming voltage, current density, electrolyte properties (concentration, ion content, and pH), temperature, circulation speed of the electrolyte, surface area ratio, and distance between the anode and cathode.[4]

Growth of Titania in the nanoporous or nanotube structure requires the current density to be in a particular range or sweetspot. [2] This current density needs to be maintained all across the dental implant and fluctuations in the current density need to be minimised in order to achieve uniform growth. As the dental implant tends to have a screw like structure, maintaining this current density becomes a challenge, especially in the grooves. In order to address this challenge, we have attempted to model the current distribution on the implant surface and understand how the uniformity of current on the surface can be improved.

# 2 Simulations

## 2.1 Setup

We used the *Primary Current Distribution (cd)* physics in the Electrodeposition Module in COMSOL Multiphysics to simulate the current distribution during anodization. The CAD for the dental implant was obtained from the GrabCAD library having dimensions summarized in Table 1. Two types of electrode geometries were chosen for this analysis - an cylindrical surface sheet electrode and an array of 1cm x 1cm electrodes. The cylindrical surface electrode was used for a preliminary analysis to calibrate the effect of inter electrode gap, while the electrode array is more suited to predict and design real-world experiments. As shown in Fig. 1, the implant is given a positive voltage (red) and the remaining electrodes are grounded (green). For both setups, meshing is set to 'physics-controlled' and refinement is set to 'extra fine' as shown in Fig. 2. Stationary studies are conducted in all cases to measure the spatial distribution of current density.

| Parameter | Value |
|---|---|
| Length | 15 mm |
| Top Diameter | 4.5 mm |
| Pitch | 0.8 mm |
| Thread Depth | 0.44 mm |
| Thread Thickness | 0.72 mm |
| Slant Angle | 8° |

**Table 1:** *Geometrical parameters of implant*

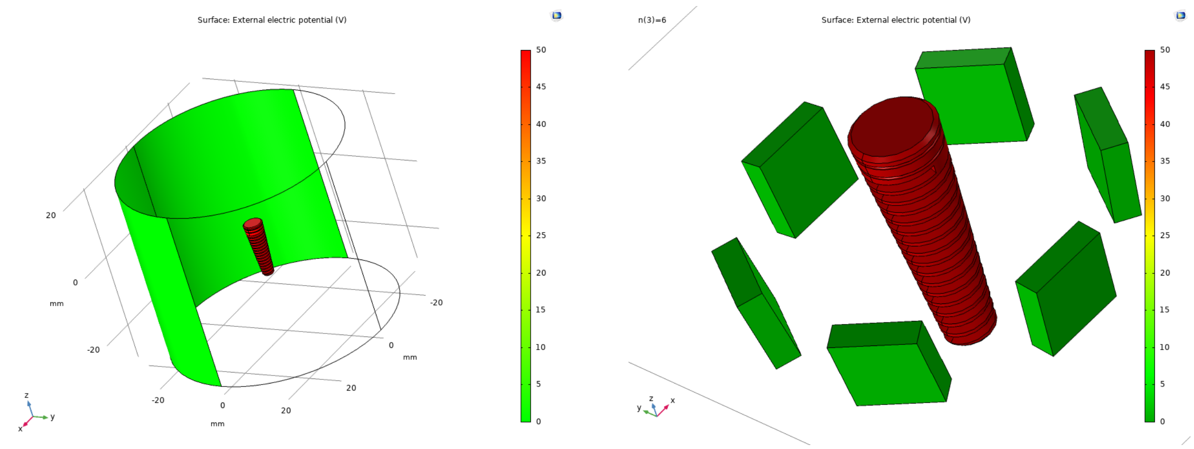


**(a)** *Cylindrical Electrode* **(b)** *Discrete Electrode*

**Figure 1:** *Electrode Setups - anode (red) and cathode (green). Flat surfaces and part of curved surface of cylinder hidden for representational purposes*

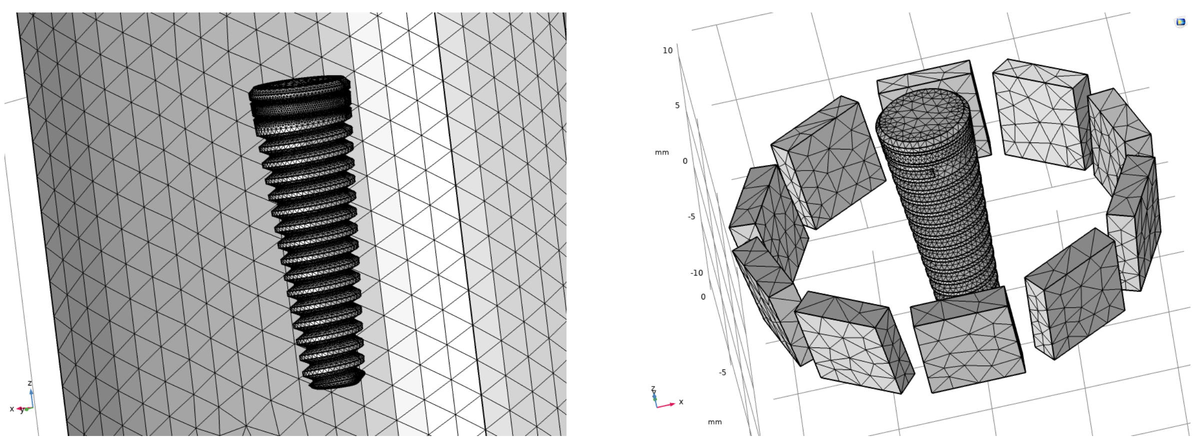

**(a)** *Cylindrical Electrode* **(b)** *Discrete Electrode*

**Figure 2:** *Meshing of Electrode Setups*

## 2.2 Cylindrical Electrode

The electrolyte region was constructed as a cylinder with height 5cm, with conductivity results obtained from literature. The setup parameters are summarized in the table below. Radius of cylinder was swept from 5 mm to 30 mm for 5V - 50V anode voltage.

| **Parameter** | **Value** |
|---|---|
| Simulation height | 5 cm |
| Conductivity | 0.873 mS/m |
| Anode Voltage (E) | 5V - 50V |
| Cylinder Radius (r) | 5-30 mm |

**Table 2**

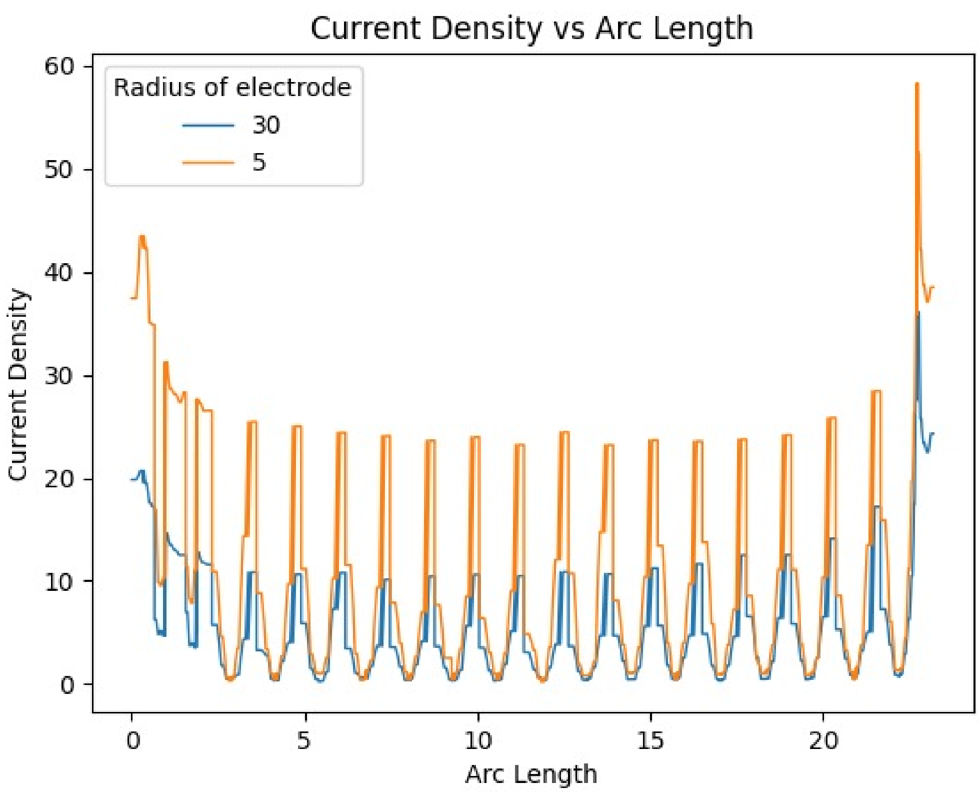


**Figure 3:** *Variation of Current Density along the edge of the implant (from top to bottom) for E = 50V*

The current density at the surface of the implant is depicted in Fig. 8. Due to the implant structure, surface of the implant has alternating maximas (on the threads) and minimas (in the valleys between the threads). This is emphasized in Fig. 3, which shows the quantitative variation of current along the length of the implant, from top to bottom. This variation in the current density at the surface is a major obstacle to achieving uniformity in the growth of nanotubes. By comparing Figures 8 and 3, we observed that the current shoots up quickly from the valley to the maxima, and stays nearly constant at the maxima. Due to this, it will not be possible to achieve a narrow current distribution over significant lengths on the slope of the threads. Additionally, the current in the valley approaches zero which makes it impossible to grow nanotubes in the vicinity of the valley. Hence, the only remaining option is to aim to obtain the ideal current values over the flat regions at the top of the threads.

We plotted a histogram of the current values (Fig. 4) in order to further quantify the distribution of current. Note that in the histograms, we excluded the extremities of the implant in order to eliminate misleading data from end effects. We compared the histogram peaks with values in Fig. 3 to gain insights on the current distribution. As expected there are two peaks- the peak at lower currents corresponds to the distribution over the slope and valley of the threads, while the second peak ($\tilde{2}5A/m^3$ for r = 5mm) corresponds to the current near the top of the threads. However there is a third peak observed between the other two, whose values ($\tilde{1}0A/m^3$ for r = 5mm) corresponds to the relaxation of the current slope in Fig. 3. It can be observed that increasing the radius or decreasing the voltage leads to lowering the values of the surface current density.

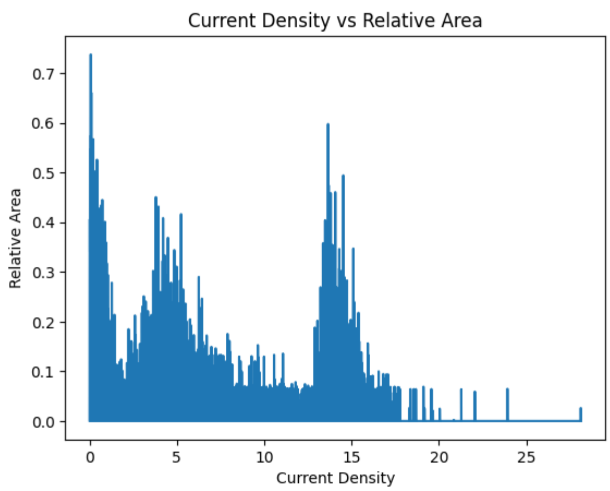


**(a)** *E = 30V, r = 5mm*

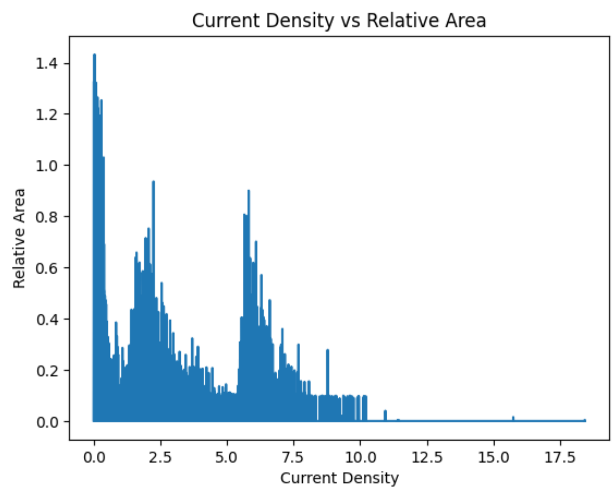


**(b)** *E = 30V, r = 30mm*

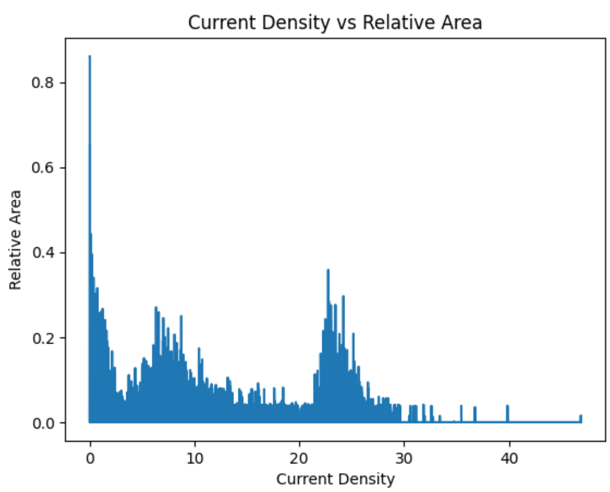


**(c)** *E = 50V, r = 5mm*

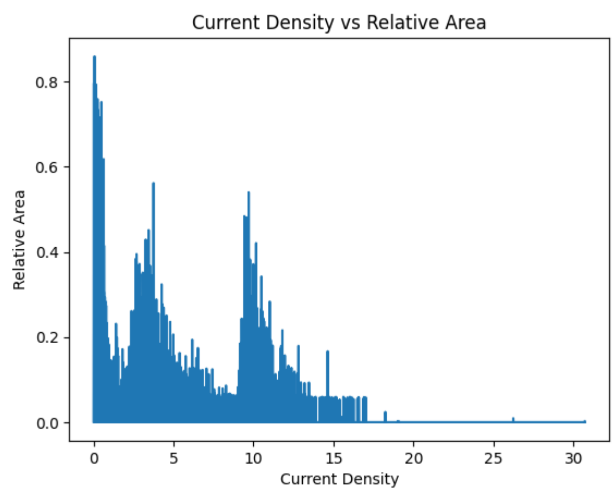


**(d)** *E = 50V, r = 30mm*

**Figure 4:** *Histograms of Surface Current density for Cylindrical electrodes*

Hence, the objective of performing these simulations would be to align the 'sweet-spot' current to the high current peak in the histogram for a geometry, and use the results as a guide for setting up the electrodes in an actual experiment. We calculated the position and full width at half maxima for the second peak and tabulated the results in Table 3. We can from both the table and the histograms that increasing the radius leads to broader peaks with lower currents. Increasing the voltage results in narrower peaks at higher voltages, but at the expense of relative area in the peak, since there will be a sharper current gradient at higher voltages. Based on literature , the sweet spot current is around 10 $A/m^3$. For our particular geometry and conductivity parameters, we have achieved a narrow peak in this range for 50V and 20-30 mm

| Voltage applied (V) | Radius (mm) | Peak Maxima | Peak FWHM |
|---|---|---|---|
| 5 | 5 | 2.275 | 0.414 |
| 5 | 7 | 1.700 | 0.517 |
| 5 | 10 | 1.432 | 0.600 |
| 5 | 13 | 1.256 | 0.545 |
| 5 | 16 | 1.159 | 0.531 |
| 30 | 5 | 13.652 | 0.065 |
| 30 | 10 | 8.592 | 0.097 |
| 30 | 15 | 6.639 | 0.110 |
| 30 | 20 | 6.639 | 0.115 |
| 30 | 30 | 5.820 | 0.120 |
| 50 | 5 | 22.754 | 0.042 |
| 50 | 10 | 14.319 | 0.061 |
| 50 | 20 | 11.064 | 0.064 |
| 50 | 30 | 9.700 | 0.057 |

**Table 3**

## 2.3 Discrete Electrode

For the discrete electrode setup, we implemented radially placed square electrodes. We observed the variation of current distribution while sweeping over the number of electrodes and their radial position. Voltage was maintained at 50V. Additionally, we attempted improving performance, by tilting the electrodes to 8°to make them parallel to the implant surface.

| Parameter | Value |
|---|---|
| Electrode side | 1 cm |
| Electrode thickness | 1.5 mm |
| Conductivity | 0.873 mS/m |
| Anode Voltage (E) | 50V |
| Setup Radius (r) | 10-20 mm |
| Number of electrodes (n) | 2 - 10 |

**Table 4**

The surface current density variation with number of electrodes is depicted in Fig. 9. Similar to the results in the previous section, it is observed that the screw topology results in repeated maximas and minimas along the length of the implant. The variation of current along the length of the implant and histograms are displayed in Figs. 5 and 7. It must be noted that even due to the small size of the eletrodes, there is still not much longitudinal variation except at the extremities. Additionally due to the lack of the radial symmetry which existed in the previous setup, there is a variation in the radial current distribution as shown in Fig 6. Hence, it has now become a matter of optimizing the longitudinal uniformity, as well as the radial uniformity.

Note that in the histograms, we excluded the extremities of the implant in order to eliminate misleading data from end effects. Unlike the previous section, the histograms exhibit a more bimodal distribution. As expected, the FWHM of the second peak is significantly wider than in the cylindrical case, as seen in Table 5, largely due to the difference in heights of the electrodes. It can also be seen that for the same voltage and radius, there is an increasing current with increasing the number of electrodes, since there are more paths for conduction to take place. Tilting the electrodes do not cause much improvement in the FWHM of the peak. As seen from Fig. 6 there is an improved radial uniformity with increasing the number of electrodes. However, beyond 6 electrodes, there is not much significant improvement.

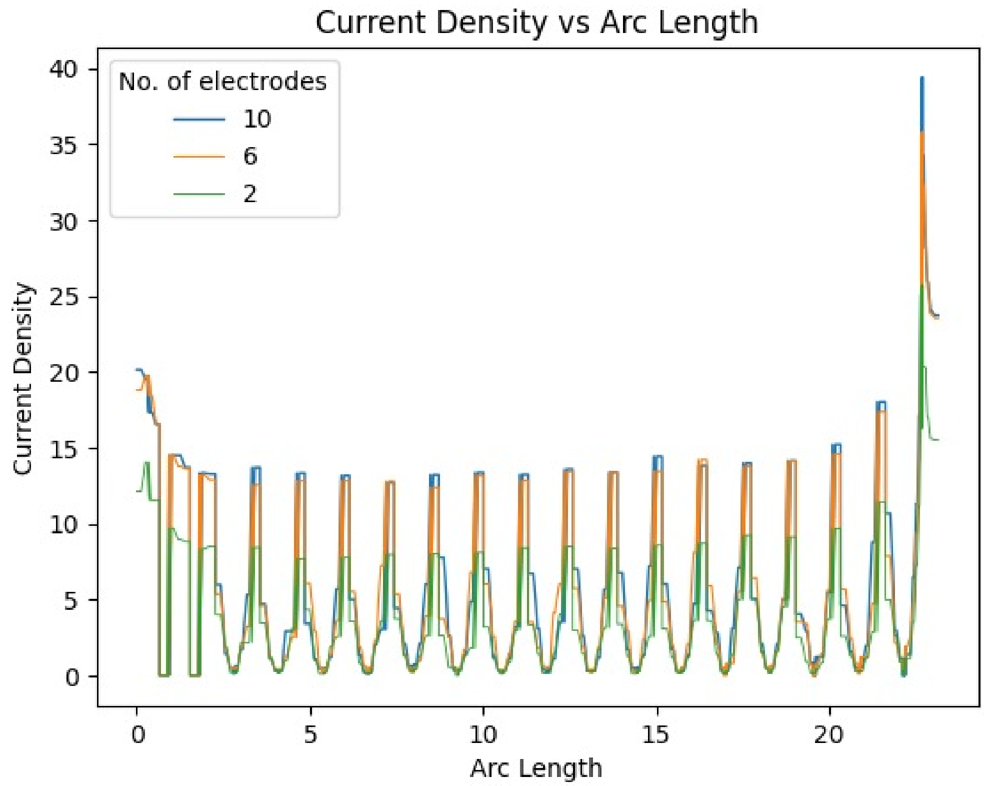


**Figure 5:** *Variation of Current Density along the edge of the implant (from top to bottom) for E = 50V and r = 10 mm*

| Radius (mm) | No. of electrodes | Peak Maxima ($A/m^3$) | Peak FWHM ($A/m^3$) |
|---|---|---|---|
| 10 mm | 2 | 8.479 | 0.104 |
| 10 mm | 4 | 11.310 | 0.087 |
| 10 mm | 6 | 10.964 | 0.088 |
| 10 mm | 8 | 11.970 | 0.093 |
| 10 mm | 10 | 11.887 | 0.077 |
| 10 mm with 8°tilt | 2 | 8.497 | 0.124 |
| 10 mm with 8°tilt | 4 | 10.602 | 0.101 |
| 10 mm with 8°tilt | 6 | 11.836 | 0.101 |
| 10 mm with 8°tilt | 8 | 11.893 | 0.076 |
| 20 | 2 | 5.819 | 0.158 |
| 20 | 4 | 7.738 | 0.121 |
| 20 | 6 | 8.486 | 0.109 |
| 20 | 8 | 8.478 | 0.105 |
| 20 | 10 | 9.042 | 0.105 |

**Table 5**

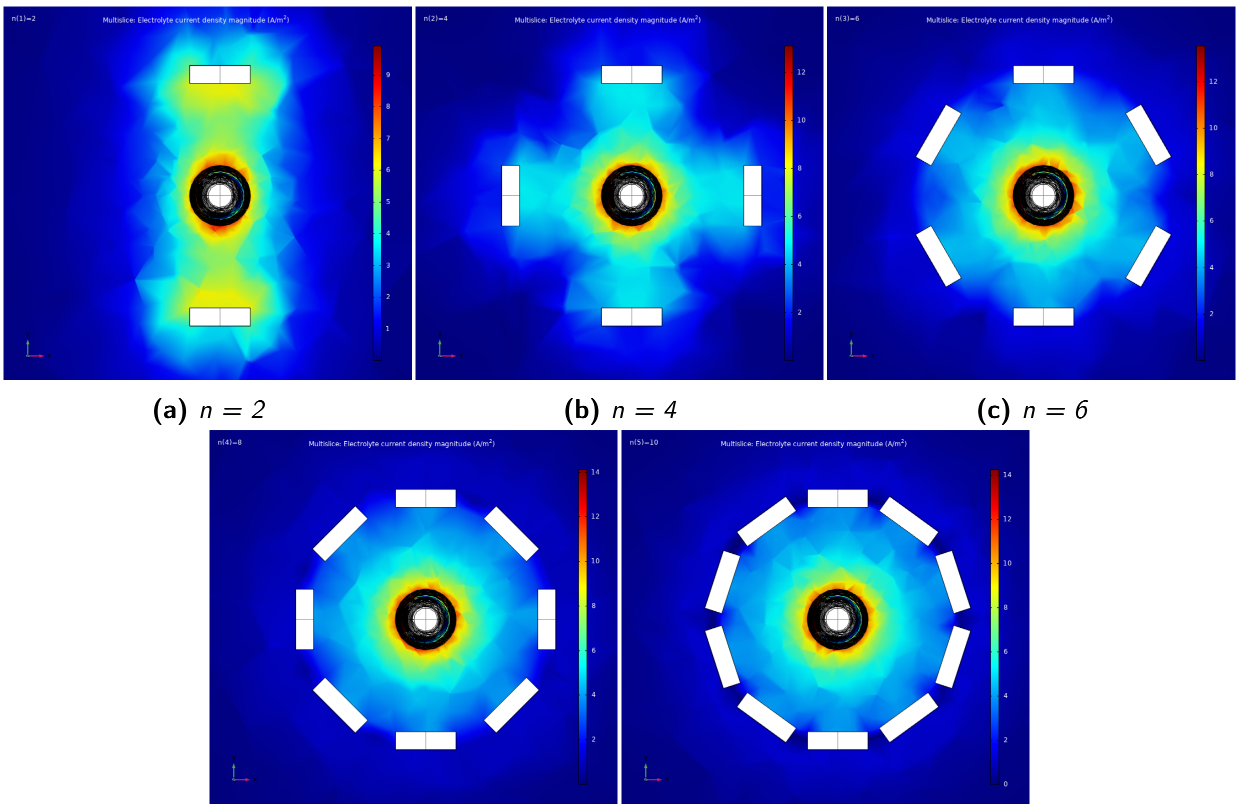


**(a)** *n = 2* **(b)** *n = 4* **(c)** *n = 6*

**(d)** *n = 8* **(e)** *n = 10*

**Figure 6:** *Electrolyte Current distribution at the mid-plane for E = 50 V and r = 10 mm*

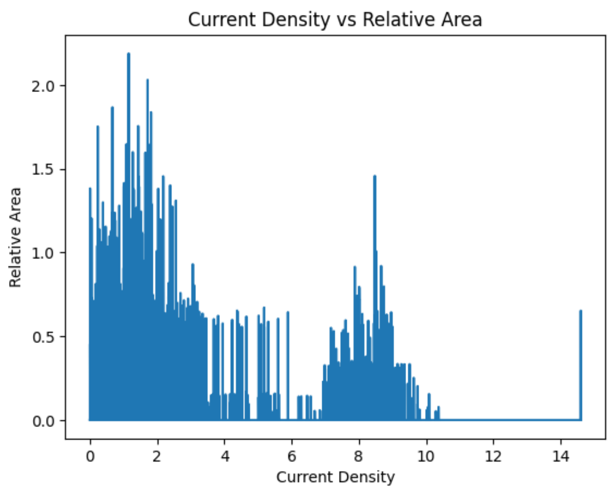


**(a)** *n = 2*

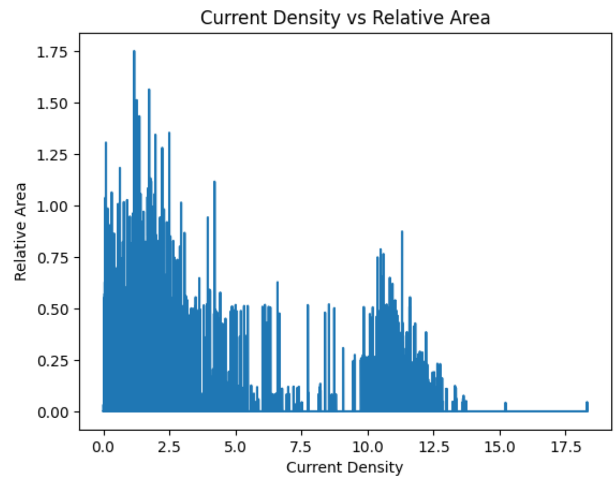


**(b)** *n = 4*

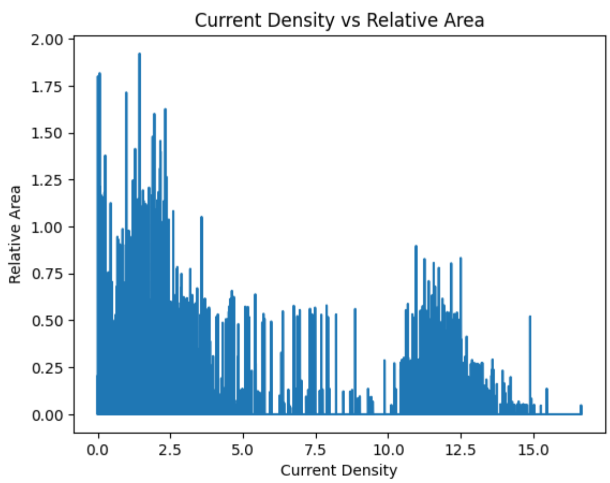


**(c)** *n = 6*

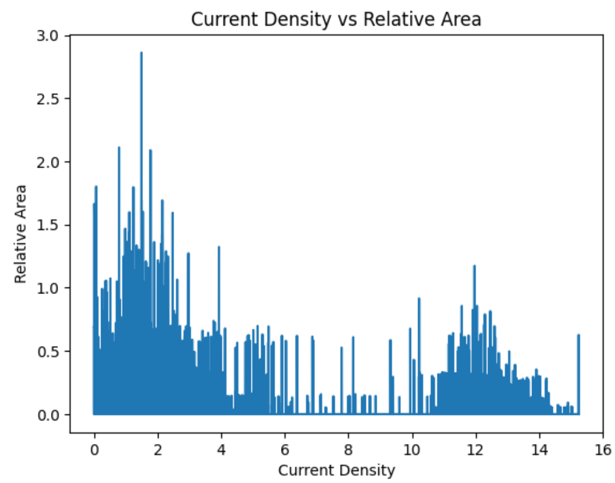


**(d)** *n = 8*

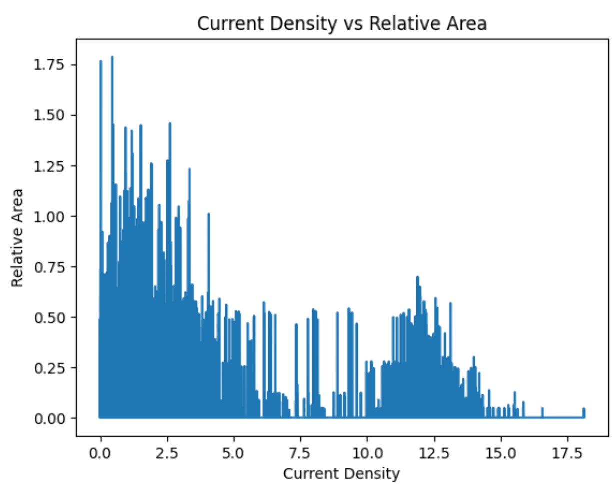


**(e)** *n = 10*

**Figure 7:** *Histograms of Surface Current density for E = 50 V and r = 10 mm*

# 3 Conclusions

Our simulations have led to useful insights about the way that current is distributed for over this implant geometry and can can be implemented to obtain better uniformity of nanotube growth.

1. Our simulations show that there is an almost zero current at the valleys between the threads regardless of the voltage and radius. Moreover, there is a sharp jump in current along the walls of the threads, eventually staying constant on the surface of the threads. Hence, it will not be possible to obtain a uniform current over the entire implant surface.

2. Current density histograms show a bimodal distribution for discrete electrode setups.The broad peak at lower currents corresponds to the valleys whereas the narrower peaks with higher current corresponds to the ridges.

3. The analysis shows that the only region where current is uniform over significant length scales, is the flat tips of the threads. Hence, it is optimal to aim obtaining the 'sweet-spot current' over here.

4. Using shorter discrete electrodes does not adversely effect the longitudinal distribution of the current on the implant surface.

5. While using a discrete electrode setup, there is a clear improvement in symmetry of current distribution with increasing number of electrodes. However, increasing the electrodes beyond 6 is cumbersome and does not significantly improve the current distribution at these radii. Additionally, implementing a tilt also does not significantly improve the uniformity.

6. At the same time, these results also give insights on designing implant structures specifically for nanotube growth. The design can be optimized to have larger areas of flat surface at the top of the threads.

# Bibliography


[1] K Indira, U Kamachi Mudali, and N Rajendran. "Corrosion behavior of electrochemically assembled nanoporous titania for biomedical applications". In: *Ceramics International* 39.2 (2013), pp. 959–967.

[2] Zainovia Lockman et al. "Influence of anodisation voltage on the dimension of titania nanotubes". In: *Journal of Alloys and Compounds* 503.2 (2010), pp. 359–364.

[3] NA Al-Mobarak and AA Al-Swayih. "Development of titanium surgery implants for improving osseointegration through formation of a titanium nanotube layer". In: *International Journal of Electrochemical Science* 9.1 (2014), pp. 32–45.

[4] Young-Taeg Sul. "Electrochemical growth behavior, surface properties, and enhanced in vivo bone response of TiO2 nanotubes on microstructured surfaces of blasted, screw-shaped titanium implants". In: *International journal of nanomedicine* (2010), pp. 87–100.

[5] Nathan Swami, Zhanwu Cui, and Lakshmi S Nair. "Titania nanotubes: novel nanostructures for improved osseointegration". In: (2011).

## Additional Figures

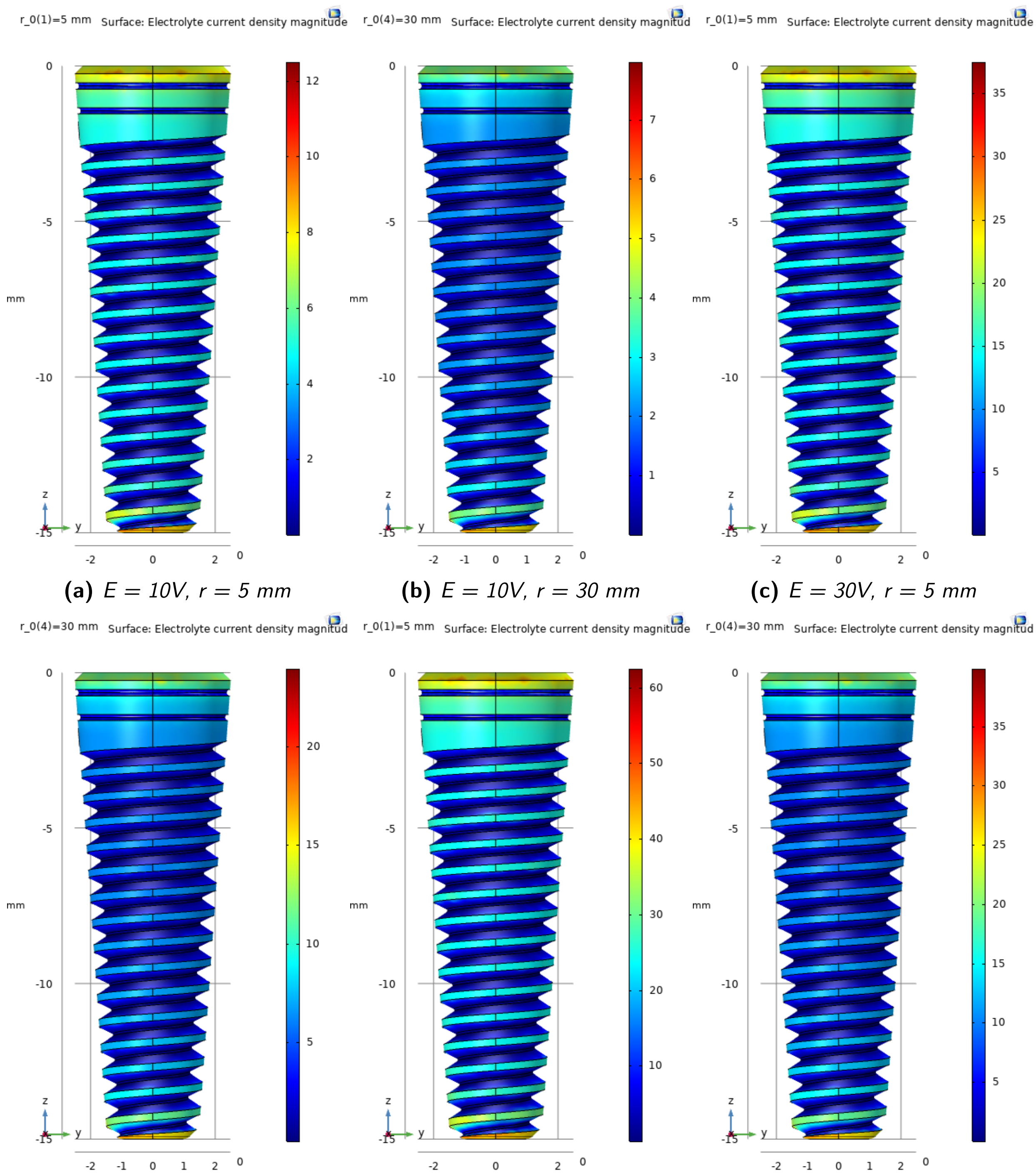


**(a)** *E = 10V, r = 5 mm*

**(b)** *E = 10V, r = 30 mm*

**(c)** *E = 30V, r = 5 mm*

**(d)** *E = 30V, r = 30 mm*

**(e)** *E = 50V, r = 5 mm*

**(f)** *E = 50V, r = 30 mm*

**Figure 8:** *Distribution of current density at surface of the electrode in the cylindrical setup*

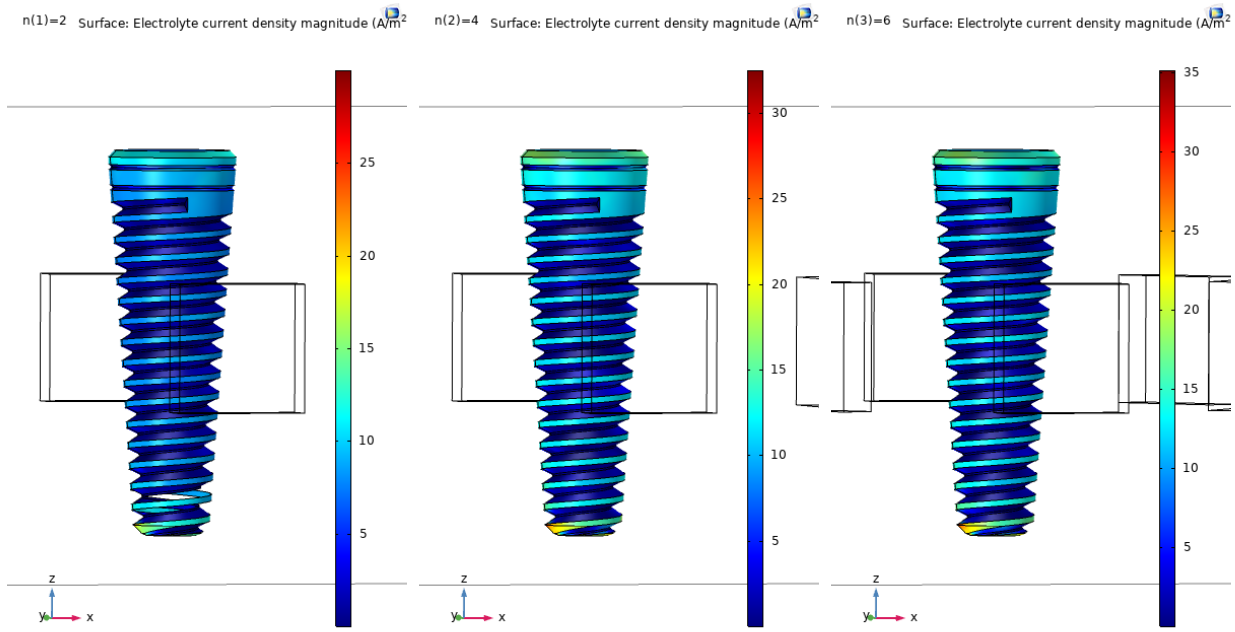


**(a)** *n = 2* **(b)** *n = 4* **(c)** *n = 6*

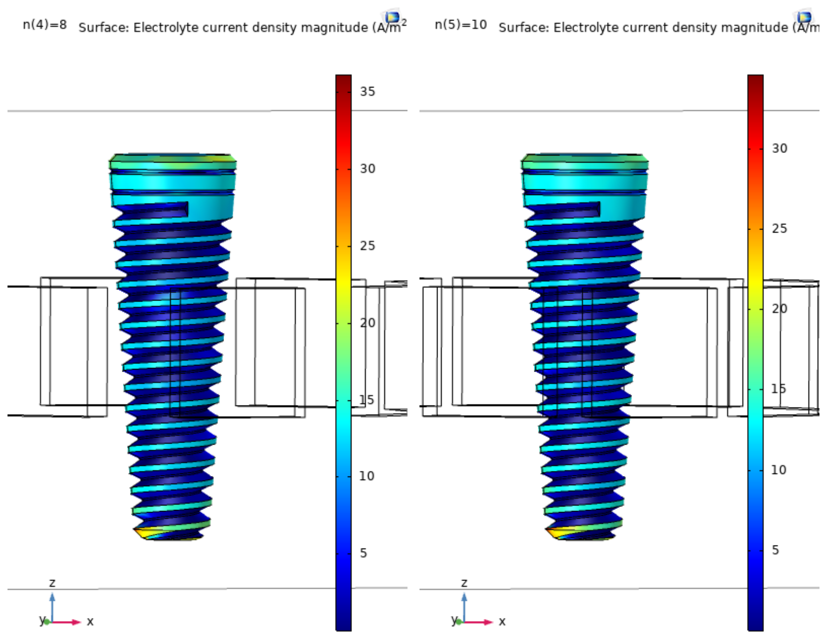


**(d)** *n = 8* **(e)** *n = 10*

**Figure 9:** *Distribution of current density at surface of the implant in the discrete electrode setup for E = 50V and r = 10mm*